Research Article

Paloma Serrano-Díaz, David W. Williams, Julio Vega-Arreguin, Ravichandran Manisekaran, Joshua Twigg, Daniel Morse, René García-Contreras, Ma Concepción Arenas-Arrocena, and Laura Susana Acosta-Torres*

Geranium leaf-mediated synthesis of silver nanoparticles and their transcriptomic effects on *Candida albicans*

https://doi.org/10.1515/gps-2022-8105
received September 01, 2022; accepted January 11, 2023

Abstract: *Candida albicans* is the most predominant fungal species isolated from medical devices, including catheters, heart valves, and dental prostheses. In recent years, it has been demonstrated to be resistant to many antifungals; therefore, silver nanoparticles (AgNPs) have been proposed as an alternative. But only a handful of research is contributed to omic-based studies to study the various impacts of AgNPs on *Candida* species and other microorganisms. Thus, the study aims to biosynthesize AgNPs using *Pelargonium-hortorum* leaf and test its antifungal, cytotoxicity, and global gene expression on *Candida* through transcriptomic profiling. The leaf-assisted AgNPs resulted in spherical shapes with a particle size of 38 nm. The anticandidal effect demonstrated that the Minimum inhibitory concentration was 25 $\mu g \cdot mL^{-1}$. Later, the cytotoxicity assay reported a moderate impact on the human gingival fibroblast cells. Finally, the transcriptomic analysis demonstrated the differential gene expression of 3,871 upregulated and 3,902 downregulated genes. Thus, proving the anticandidal effect of AgNPs on *Candida* through RNA-seq experiments and the regulated genes is highly important to cell wall integrity, adherence, and virulence.

Keywords: green synthesis, silver nanoparticles, antifungal activity, transcriptomics, RNA-sequencing

1 Introduction

Candida albicans (*C. albicans*) is a unique and opportunistic pathogen that frequently dwells in equilibrium with other microorganisms of the commensal mucosal microbiota. However, it is considered a critical resourceful, highly organized yeast causing various forms of candidiasis in immunocompromised patients [1]. In the case of a healthy individual, the balance between the host, *C. albicans*, and the commensal microbiota is maintained. It is due to the complex and dynamic interplay between various immune and environmental factors, such as pH and nutrient availability [2]. But the presence of removable dental prostheses, medications like antimicrobials, and behavioral factors such as smoking can cause a variation, affecting the regulatory elements. This may lead to an altered microbial community, which could cause the rapid proliferation of *C. albicans*, resulting in local and systemic infections [3].

In general, healthy individuals have 20–40% of *C. albicans* colonization prevalence in the oral cavity, whereas over 60% in immunocompromised subjects, which can pose a severe risk of infection. *C. albicans* is the most

* **Corresponding author: Laura Susana Acosta-Torres,** Interdisciplinary Research Laboratory (LII), Nanostructures and Biomaterials Area, Escuela Nacional de Estudios Superiores Unidad León, Universidad Nacional Autónoma de México, Predio el Saucillo y el Potrero, Comunidad de los Tepetates, 37684, León, Mexico, e-mail: lacosta@enes.unam.mx
Paloma Serrano-Díaz: Universidad Nacional Autónoma de México, Av. Universidad 3004, Copilco Universidad, Coyoacán, 04510 Ciudad de México, CDMX, Mexico; Interdisciplinary Research Laboratory (LII), Nanostructures and Biomaterials Area, Escuela Nacional de Estudios Superiores Unidad León, Universidad Nacional Autónoma de México, Predio el Saucillo y el Potrero, Comunidad de los Tepetates, 37684, León, Mexico
David W. Williams, Joshua Twigg, Daniel Morse: School of Dentistry, College of Biomedical and Life Sciences, Cardiff University, Cardiff, United Kingdom
Julio Vega-Arreguin: Agri-Genomics Laboratory, Interdisciplinary Research Laboratory (LII), National School of Higher Studies (ENES) León Unit, Predio el Saucillo y el Potrero, Comunidad de los Tepetates, 37684, León, Mexico
Ravichandran Manisekaran, René García-Contreras, Ma Concepción Arenas-Arrocena: Interdisciplinary Research Laboratory (LII), Nanostructures and Biomaterials Area, Escuela Nacional de Estudios Superiores Unidad León, Universidad Nacional Autóde los Tepetates, 37684, León, Mexico

prevalent fungal species isolated from different medical devices, including catheters, pacemakers, heart valves, joint prostheses, contact lenses, and dental prostheses. The continuous mistreatment of *C. albicans* infection causes antifungal resistance, an emergent problem despite a diverse range of antifungals exploiting different mechanisms of action against fungi. The most frequently used antifungal agents are azoles, polyenes, echinocandins, and nucleoside analogues. Nonetheless, *C. albicans* biofilms are resistant to most antifungals compared to their planktonic counterparts [4,5].

Azoles, for example, are ineffective against the biofilms of *C. albicans* [6]. To overcome the limitations and drawbacks of traditional antifungal agents, novel antifungals must be developed to combat biofilm-based infections. With the booming development of nanotechnology, versatile nanoscale materials with antimicrobial effects have been designed and exploited against several infections, i.e., nano-antimicrobials (n-AMBs). Nanoparticles (NPs) present a diverse biocidal activity mechanism that is very different from traditional antibiotics. Nanostructured materials have unique physicochemical properties such as their controllable size, large surface area, high reactivity, individual biological interactions, and functional structures [7]. Thus, n-AMBs are considered a promising and outstanding alternative in deciphering the problem of microbial resistance [8]. In most cases, n-AMBs are in metallic form with a nanometric size that facilitates the internalization of the microorganisms, thereby controlling the proliferation by intervening in the biological mechanisms [9].

The outcome of the n-AMBs area has resulted in an enormous number of metallic NPs effective against several microorganisms [10]. One such spectacular NP that is investigated widely is AgNP synthesized by different sources and tested its potential against bacteria, fungi, and viruses [11]. These led to the emergence of numerous products in the market for human use. Even though extensive research has been reported, the antimicrobial mechanism of AgNPs is not fully understood. Overall, it is known that Ag^+ ions bind to proteins and nucleic acids that are negatively charged, causing structural changes and deformations [12]. These ions are responsible for forming reactive oxygen species (ROS), primarily affecting the cell membrane through the peroxidation of polyunsaturated phospholipids in a contact-dependent manner in regard to tackling *C. albicans* and other microorganisms from different origins, various reports have been documented [13,14]. However, the essence of AgNPs toxicity still lacks in-depth studies, i.e., on a molecular level. For example, our search found that very few articles represented in Table 1 [15–21] have made an omic-based analysis in specific transcriptomics. The genetic information encrypted in the cell nucleus is expressed through transcription and translation mechanisms [22]. The transcription process depends on the intra/extracellular stimulus that leads to both the expression and repression of genes. Some sophisticated tools have made it possible to study the transcriptomic profile of *C. albicans* using next-generation sequencing (NGS) technologies, such as RNA-seq [23]. The impact of the stimulus's mechanism of action can be studied by analyzing the differentially expressed genes.

Thus, the current research project aims to obtain AgNPs using green technology and evaluate their biological response. Even though every year several studies are conducted based on AgNPs for various biomedical applications, especially antifungal agent against various strains. But many studies have created a void on a effect on cellular/molecular level. Thus, in this research, we have made a comprehensive analysis to fulfill various aspects. Thus, apart from routine testing like cytotoxicity, and antifungal studies, most importantly, gene expression profiling through transcriptomic mediated technique against *C. albicans* by RNA-sequencing method has been carried out to determine both the up- and downregulation of genes which are affected during the exposure of AgNPs represented in Scheme 1.

2 Materials and methods

All the chemical reagents were purchased from Sigma-Aldrich™, Mexico, until otherwise mentioned and used without any further modifications.

2.1 AgNPs synthesis

Through chemical synthesis, AgNPs were synthesized using silver nitrate ($AgNO_3$, purity ≥99.0%) as a precursor and a filtered *Pelargonium-hortorum* infusion as a reducing and stabilizing agent. The $AgNO_3$ precursor solution was prepared at a molar concentration of 25 mM and dissolved in 20 mL of deionized water (DIw). For the preparation of leaf extract, 12 g of *Pelargonium* tender leaves were weighed, rinsed, and boiled in 100 mL of DIw for 5 min at a temperature of 95°C. Before the synthesis, leaf extract was primarily filtered through 0.2 µm thick Whatman® filter paper. Initially, 20 mL of ethylene glycol was added to a three-neck flask and heated at 185°C; 10 mL of *Pelargonium* extract was mixed for 5 min. Subsequently, the $AgNO_3$ solution was added dropwise

Table 1: Investigations that studied the impact of AgNPs against different microorganisms through transcriptomic profiling

Reference	NPs size (nm)	Microorganisms
Liu et al., 2017 [15]	6–20	*Candida albicans*
Zheng et al., 2018 [16]	20–30	*Paracoccus denitrificans*
Piersanti et al., 2021 [17]	14.6	*Tetrahymena thermophila*
Sun et al., 2017 [18]	5–10	*Escherichia coli* and *Staphylococcus aureus*
Singh et al., 2014 [19]	7–20	*Pseudomonas aeruginosa*
Horstmann et al., 2019 [20]	20	*Saccharomyces cerevisiae*
Masri et al., 2021 [21]	100–125	*Escherichia coli* K1

every 2 min until a color change was noticed to amber yellow and continued for 90 min to ensure complete reduction of the precursor. Finally, the reaction is allowed to cool down to room temperature and washed twice through centrifugation for 10 min at 4,600 rpm. The pellet is dispersed in a sterile DIw and stored at 4°C until further use for characterization and application studies.

2.1.1 Characterization

The leaf-assisted AgNPs synthesis was confirmed using UV-visible (UV-Vis) spectroscopy (Multiskan GO, Thermo Scientific, Massachusetts, USA), measured in the 200–1,000 nm range. The morphology and size were determined using transmission electron microscopy (TEM, JEOL-1010, JEOL, Massachusetts, USA), where the NP sample was loaded onto a 200 mesh carbon-coated copper grid (Ted Pella, Inc, California, USA). The functional groups of both leaf infusion and synthesized AgNPs were analyzed using Fourier-transform infrared spectroscopy (FTIR, Bruker Tensor-27, California, USA), from 4,000 to 400 cm^{-1} in a transmission mode with a resolution of 4 cm^{-1}. The particle size and surface charge were characterized using Zetasizer Nano ZS90 Size Analyzer (Malvern Panalytical, Malvern, UK) using folded capillary cell cuvettes.

2.2 Antifungal activity

2.2.1 Candida growth

The antifungal effect of AgNPs was tested using two separate experiments, such as microdilution and colony-forming unit methods. *C. albicans* ATCC 90028 (Virginia, USA) was cultured aerobically at 37°C on Sabouroad Dextrose Agar (SDA, NutriSelect® Plus) for 24 h. A single colony was cultured overnight in a Roswell Park Memorial Institute (RPMI) 1640 medium (without glutamine, with red phenol, buffered to pH 7.0 using MOPS). A standard inoculum

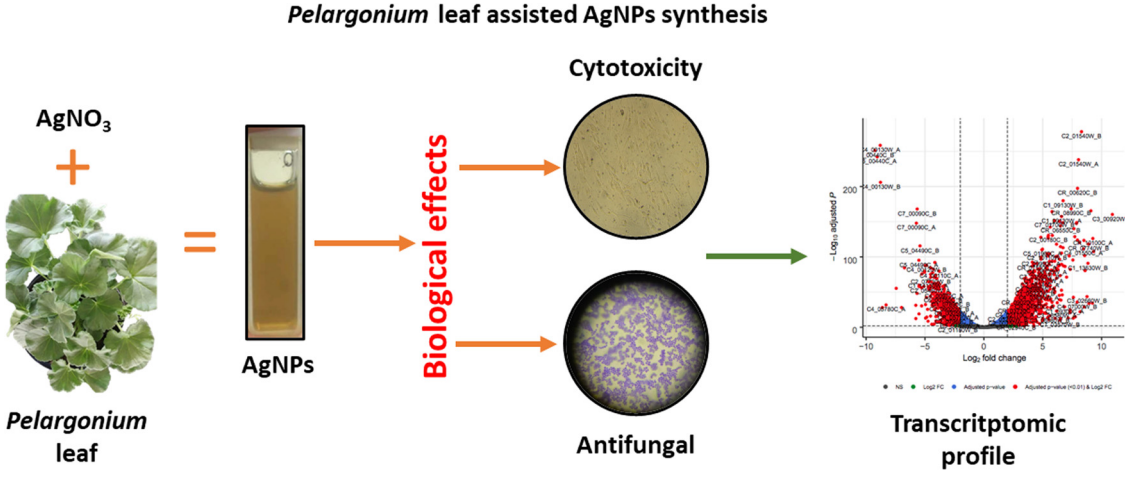

Scheme 1: Green synthesis of silver nanoparticles using *Pelargonium* leaf extract and tested its various biological effects, such as cytotoxicity on fibroblasts cells, anticandidal effect, and finally assessed the global gene expression through transcriptomic profiling on *C. albicans*.

was prepared using a densitometer (Grant Instruments™, DEN-1, Cambridgeshire, UK) at optical density (OD) 600 nm, equivalent to 1×10^7 CFU·mL^{-1}. This inoculum was then diluted at 1:1,000 to have the final working concentration of 1×10^4 CFU·mL^{-1} for further experiments.

2.2.2 Microdilution experiment

In a 96-well plate, two-fold serial dilutions of test AgNPs were prepared from 6, 12, 25, 50, 100, and 200 µg·mL^{-1}. 100 µL was added to triplicate wells, followed by an equal volume of test *Candida* suspension. The RPMI medium (without AgNPs plus *Candida*) and culture media were used as positive and negative controls, respectively. All the suspensions were then incubated for 24 h at 37°C. Then, the absorbance was measured by OD using a spectrophotometric plate-reader (FLUOstar® Omega, BMG Labtech, Inc., Bucks, UK). An absorbance reduction of at least 80% compared to positive control was considered to be indicative of *Candida* growth inhibition.

2.2.3 Colony counting method

After 24 h, 100 µL of the different concentrations tested was added into a sterile tube with 1 mL of PBS. The tubes were vortex for 1 min. Serial dilutions of 9:1 were made and cultured on an SDA-coated petri dish for 24 h, and the colonies were checked to determine the colony growth visually.

2.2.4 *Candida* morphological analysis

After 24 h, AgNPs untreated and treated samples were obtained and observed under a scanning electron microscope (SEM, Tescan Vega 3, Tescan Ltd, California, USA). They were fixed in 3% glutaraldehyde for 2 h and rinsed thrice. The dehydration process was made using 50%, 70%, 90%, and 100% ethanol concentration series. Then, hexamethyldisilazane treatment was added to the samples and kept on a fume hood overnight. Finally, the samples were sputter coated (K650x sputter coater, Quorum Technologies, Lewes, UK) with gold and analyzed in the microscope.

2.3 MTT assay on HGF cells

The reduction of the bromide salt of 3-(4,5-dimethylthiazol-2-yl)-2,5-diphenyltetrazole (MTT) test was used to determine the cytotoxic activity of AgNPs on human gingival fibroblasts-1 (HGF-1) cell line ATCC CRL2014 and primary culture (HGF). All cell culture reagents mentioned below were bought from Gibco™, Thermo Fisher Scientific, USA. The cell density equivalent to 1×10^5 cells·mL^{-1} was placed in a 96-well plate (100 µL) in Dulbecco's modified eagle medium (DMEM), which was previously supplemented with 10% fetal bovine serum, 1% glutamine (Glutamax), and 2% of antibiotics. The cells were incubated for 48 h at 5% CO_2 at 37°C. Then, serial dilutions of AgNPs (0–1.62 µg·mL^{-1}) were inoculated and incubated for 24 h under the same conditions. After 24 h, the medium was removed, and the freshly prepared MTT bromide salt at a concentration of 0.2 mg·mL^{-1} in supplemented DMEM was added to each well. The 96-well plate was incubated for 4 h, then, the formazan crystals were dissolved using dimethyl sulfoxide (DMSO, Karal, León, Mexico), and readings were analyzed using a Multiskan GO spectrophotometer at 570 nm. The experiment was performed in triplicates from three samples.

2.4 Transcriptomic expression profile

Total RNA extraction was performed in *C. albicans* with and without AgNPs (20 µg·mL^{-1}) treatment incubated for 24 h at 37°C using the RiboPure Yeast Kit (Invitrogen™, Massachusetts, USA) by following the manufacturer's protocol. From a 24 h grown culture in SDA, three colonies were placed in three flasks with 5 mL of SDA. Subsequently, they were incubated at 37°C under stirring at 170 rpm for 24 h. Two groups were prepared: (1) *C. albicans* control group and (2) *C. albicans* experimental group (AgNPs treated). Both the quality and quantity of RNA were estimated by measuring the absorbance at 260 and 280 nm by UV spectroscopy and using NanoDrop2000™ (Thermo Fisher Scientific Inc, USA) by placing 1 µL of each sample.

2.4.1 RNA-seq analysis

To explore the impact of the AgNPs exposure on *C. albicans*, we performed RNA-seq using NextSeq 500 system (Illumina, Inc, California, USA), where 2×75 cycles pair-end readings were conducted, and 60 million reads were obtained. The process is as follows: 2 µg of extracted RNA was dispersed in 50 µL of RNase-free water (Invitrogen™, Massachusetts, USA), and the analysis was carried out on the system. The samples were sequenced in triplicates; the generated reads were mapped to the *Candida* 5,314 genome. The statistical analysis of differentially expressed

genes was performed using edgeR software with a two-fold change and a *P*-value of <0.01.

3 Results

3.1 Synthesis and characterization

To confirm the synthesis of AgNPs, UV-Vis spectroscopy measurements (Figure 1) were carried out that indicate the presence of two distinct peaks. The peak is at 275 nm, and another maximum absorbance is at 420 nm – also the color changes of the precursor solution change to amber yellow. Then the morphology was studied using TEM (Figure 2a), representing a nearly spherical structure. The histogram in Figure 2b depicts the average particle size distribution calculated using ImageJ software and results in a size range of 30–50 nm. We also determined the hydrodynamic diameter and zeta potential of AgNPs shown in Figure 2c and d. The data indicate that the diameter was seen in a bimodal distribution of 48.77 and 176.4 nm. The surface charge was found to be –12.3 mV. The functional groups of both the leaf extract and the as-synthesized AgNPs were obtained by FTIR spectrum, which is shown in Figure 3, which depicts the bands located at 1,387, 1,630, 2,184, and 3,418 cm^{-1} in both the cases with a minor shift in point of AgNPs while comparing with the extract spectra.

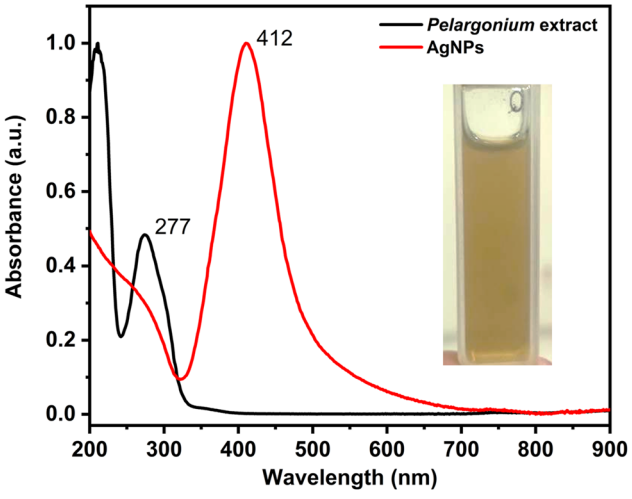

Figure 1: Represents the optical study of *Pelargonium* extract and synthesized AgNPs using UV-Vis spectroscopy (inset: shows the color of AgNPs after being reduced by *Pelargonium* extract).

3.2 Antifungal activity against *C. albicans*

The antifungal activity for AgNPs with different concentrations against *C. albicans* is represented in Figures 4 and 5. From the microdilution experiment, we found that the minimum inhibitory concentration (MIC) was 25 $\mu g \cdot mL^{-1}$, and the subsequent concentration inhibited the fungal growth to its maximum. While in colony counting, the concentrations range from 6–25 $\mu g \cdot mL^{-1}$, where *C. albicans* growth is seen. And interestingly, no colonies were identified for concentrations such as 50–200 $\mu g \cdot mL^{-1}$. The control positive was saturated with fungal growth, which becomes uncountable compared to treated samples.

Based on the effect, SEM observations are shown in Figure 6 to determine the morphology of the *C. albicans* treated with AgNPs (25 $\mu g \cdot mL^{-1}$). Indeed, there are morphological changes, resulting in deformations and irregularity of membrane (indicated with red arrows) compared to the control group, which looks smooth and with a stable cell wall surface.

3.3 Cytotoxicity on fibroblasts

Figure 7 corresponds to the MTT assay, and the graph compares the cytotoxicity effect of AgNPs on the two HGF cells. Both cases show a cytotoxic effect in a dose-dependent manner. But from the graph, we found that HGF no CC_{50} and HGF-ATCC was 1.05 $\mu g \cdot mL^{-1}$, and a hormesis effect was observed with almost all the concentrations of more than 50% cell viability.

3.4 Transcriptomic expression profile of *C. albicans*

Raw sequencing reads were filtered to remove low-quality reads using trimmomatic before subsequent analysis. Three biologically independent samples were analyzed for each condition by RNA-seq. The control group (without AgNPs treatment) obtained 28,503,316 reads for the experiment (92.88% of total reads). For the experimental group (AgNPs treatment), 30,430,674 reads were obtained (91.57% of total reads). The data were mapped to *C. albicans* SC5314. The biological replicates were very close, as shown in Figure 8a.

The volcano plot indicates upregulated and downregulated genes under the two conditions; each dot represents an individual gene's statistical significance (*P*-value) versus the magnitude of change (fold-change). Most upregulated genes are toward the right all of which are involved in

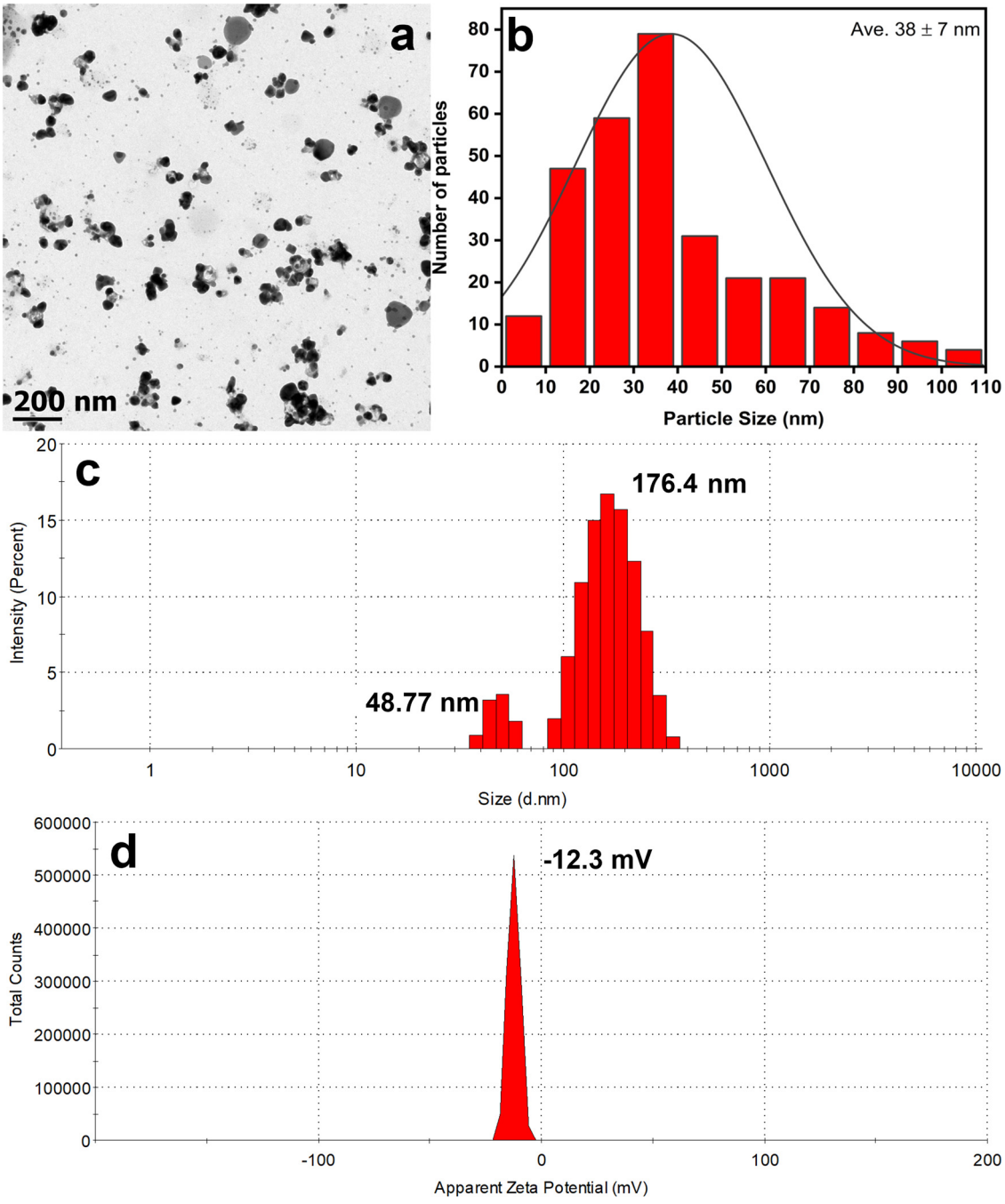

Figure 2: (a) AgNPs morphological study using TEM, which is spherical. (b) Histogram of particle size distribution calculated using ImageJ. (c) Hydrodynamic diameter of AgNPs shown in a bimodal distribution. (d) Zeta potential of as-synthesized NPs.

ergosterol and diacylglycerol biosynthesis. The most downregulated genes are on the left, with regard to *C. albicans* adherence and virulence genes (Figure 8c).

Heatmap from Figure 8c shows the hierarchical clustering of the 500 most differentially expressed genes reported by edgeR analysis according to fold-change. Red indicates higher gene expression levels, while beige indicates lower expression by reads per kilobase of transcript per million reads mapped (RPKM) in both conditions. Heatmap (Figure 8c) shows hierarchical clustering and the 500 most variable expressed genes between both conditions. RNA-seq results revealed that many genes in *C. albicans* were differentially expressed after AgNPs treatment. Gene expression values were quantified as RPKM, where a total of 3,902 genes were downregulated, and 3,891 genes were upregulated. Based on the search for

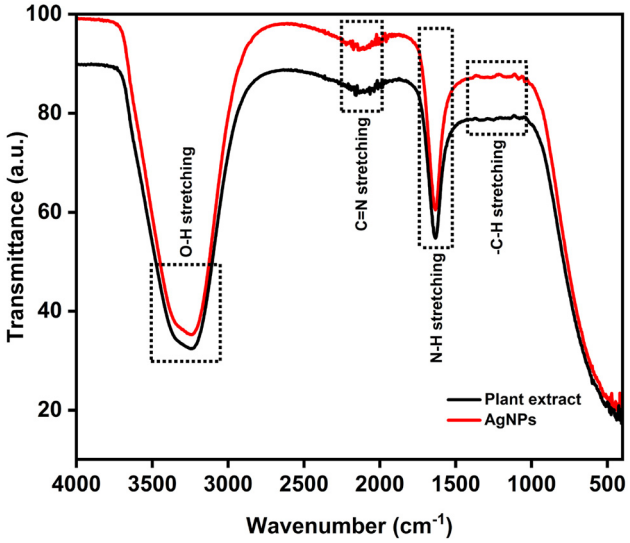

Figure 3: FTIR characterization of the *Pelargonium* extract and synthesized AgNPs indicating the various functional groups.

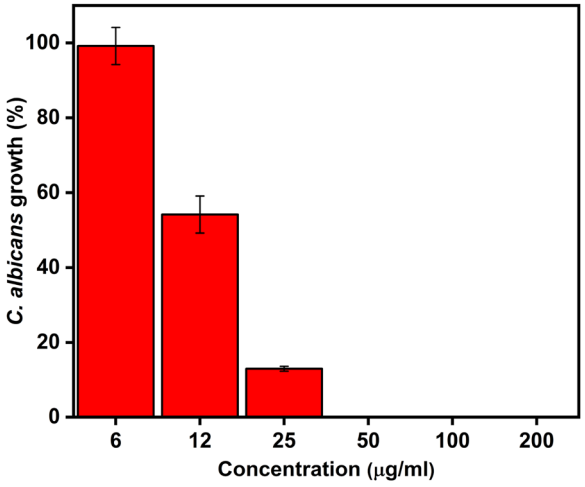

Figure 4: Antifungal studies using the microdilution method, and the graph shows the dose-dependent effect (n = 36).

differential expressions on genes widely reported in the literature, we found that these genes are essential for developing *C. albicans* biofilm formation, adhesion, pathogenicity, and virulence represented in Table 2.

4 Discussion

AgNPs and their function as an antimicrobial application have become indispensable in n-AMBs resulting in various forms to tackle different kinds of *Candida* species [24,25]. More research is carried out every day to treat *C. albicans* infections, as it is one of the life-threatening microorganisms. Multiple studies have been published in the past 5 years regarding treating *C. albicans* with AgNPs, as shown in Table 3 (some examples are listed). A common practice of AgNPs synthesis is exploiting different natural constituents to decrease the toxic effect and have synergistic mechanisms. Even though the results are promising broadly but lack the concept of explaining on a cellular level; thus, this study is purposely dedicated to identifying the effect of AgNPs on the global gene expression of *C. albicans* through transcriptomic analyses.

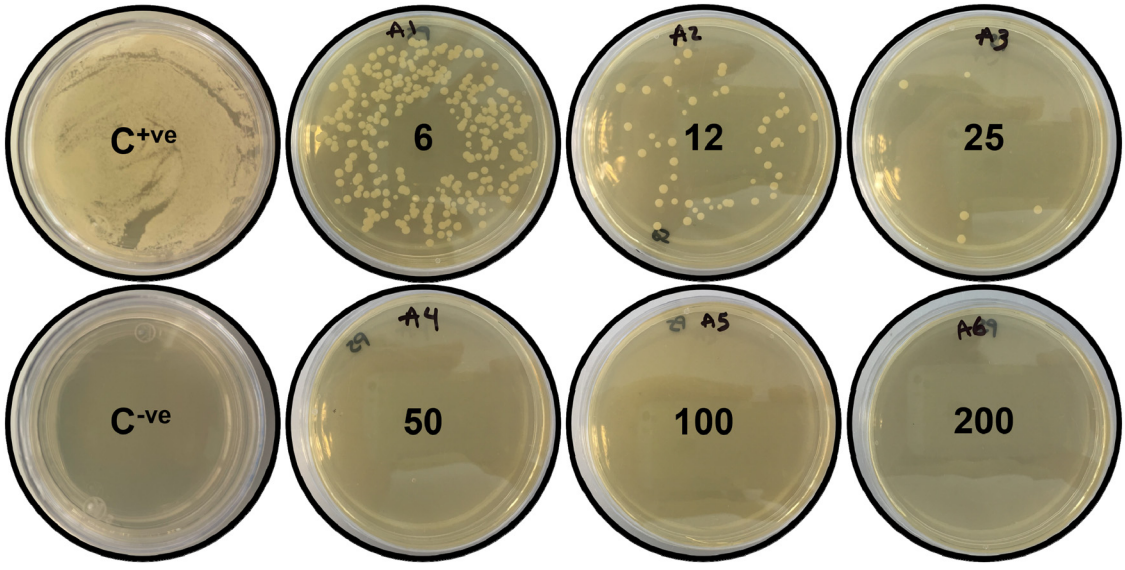

Figure 5: Shows the photos of Petri plates used for colony counting studies.

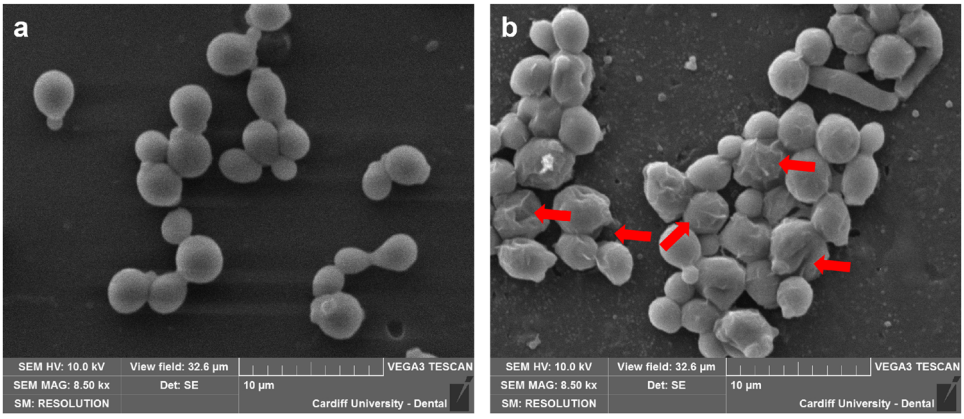

Figure 6: Morphological assessment of *C. albicans*: (a) control and (b) AgNPs treated and their effect on the fungal structure (marked in red arrows).

UV-Vis spectroscopy shows the absorbance of a pure extract with an absorbance of 277 nm, which corresponds to polyphenols [26]. These components are secondary metabolites of diverse plants resulting from a reaction to stress stimulus. Various plant extracts can reduce Ag^{+} ion to Ag^{0} due to poly hydroxyl and carboxyl groups present in these metabolites [27], Whereas the spectra for synthesized AgNPs resulted in absorbance of 410 nm, confirming the formation of NPs whose characteristic color is amber yellow [28,29]. The spectral range from 400 to 420 nm corresponds to spherical AgNPs [30], inferring a particle size between 35 and 50 nm, as reported in the literature. Also, from the spectra, the extract's intensity has been diminished to maximum, demonstrating that this group of molecules is responsible for the process of reducing AgNPs [31,32].

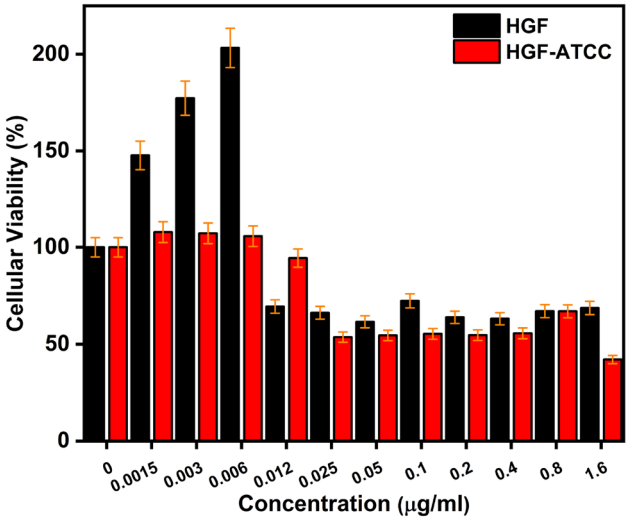

Figure 7: Cytotoxicity evaluation of HGF primary cells and HGF ATCC cell line using MTT after incubating AgNPs for 24 h (n = 36).

From the morphological analysis using TEM, nearly spherical-shaped and uniformly distributed AgNPs were found with minor organic content of the extract, which helps stabilize the NPs and avoid aggregation or clustering. The size was measured using the histogram and was found to be 30–44 nm with an average particle size of 38 nm [33,34] using ImageJ software by considering 302 particles. The analysis of hydrodynamic diameters (HDD) and zeta potential (ZP) plays a vital role in determining the interaction of NPs in biological entities. Thus, we analyzed HDD for synthesized AgNPs, resulting in dual modal particle size distribution. It is due to the medium in which the NPs are dispersed. Thus, the size is more significant when compared to TEM analysis as it is visualized in a dry state. Also, the Brownian movement significantly impacts determining NPs size when dispersed in the liquid medium. Apart from this, various biological compounds in the extract, such as proteins attachment through amino groups or cysteine residues, participated in the activity of both reducing and stabilizing agents [29,35]. The TEM analysis corroborates the obtained results [36]. The negative ZP value was determined in the case of obtained AgNPs, and the negative surface might be due to biomolecules present in the leaf extract [37]. Also, the ZP explains that the AgNPs are aggregated minorly, similar to the other reported literature using plant extracts [38].

The plant extracts are usually made of various organic reducing agents such as phenolic compounds, terpenes, polysaccharides, etc. [31,32]. So, FTIR characterization is one of the primary methods to analyze different functional groups. Thus, we employed this method to study the groups of leaf extract and AgNPs. The results show that both samples showed similar bands of flavonoids and terpenoids present in the leaves that highlight the presence of residues from the *Pelargonium* infusion – these

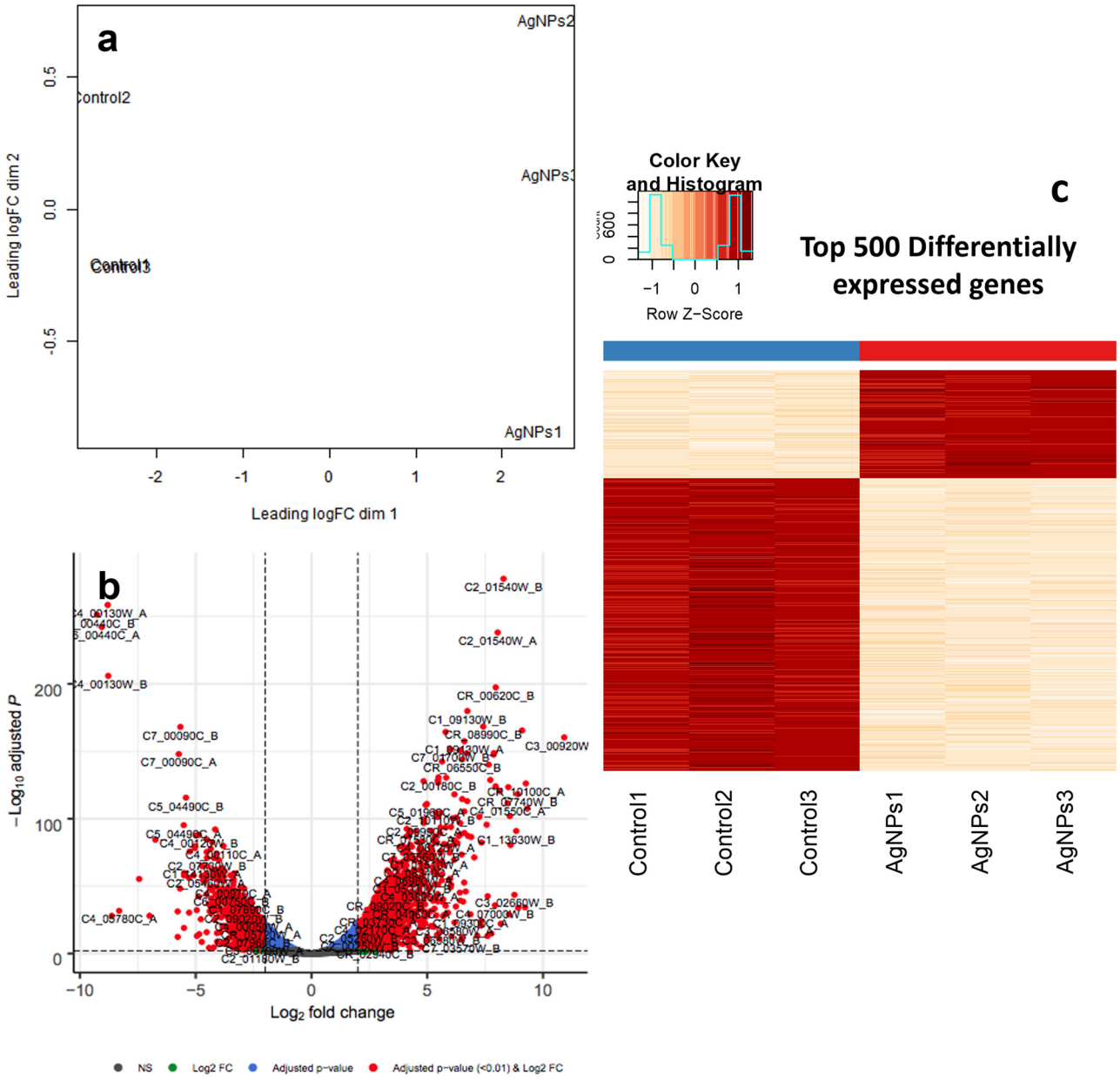

Figure 8: Transcriptome analysis of *C. albicans* by RNA-seq. (a) Multidimensional scaling plot, which determines the most significant data variation sources. (b) Volcano plots that correspond to the differentially expressed genes. Upregulated genes (red dots-right), down-regulated genes (red dots-left), no significant differential expressed genes (black dots). (c) Heat map of 500 differential gene expressions between the control group (*C. albicans* without AgNPs treatment) and experimental group (*C. albicans* treated at 25 μg·mL^{-1}).

compounds aid in stabilizing the AgNPs by attaching to the NPs on the surface [39]. This confirms that the extract's organic components are involved in reducing Ag metal. From both spectra, we found various groups with the corresponding bands ate 3,310, 2,122, 1,634, 1,385, 1,334, and 1,040 cm^{-1} [40]. The strong and sharp band at 3,310 and 1,634 cm^{-1} corresponds to alcoholic O–H and N–H stretching, respectively. The weak band at 2,122, 1,385, 1,334, and 1,040 cm^{-1} are assigned to the C═N, C–O–H bending vibration (phenolic group), –C–O stretching, and C–O stretching vibration of the OH group, which reveals the presence of phenolic compounds in the extract. In the case of AgNPs, almost similar bands are visualized but with minor shifts like 2–4 cm^{-1}, confirming that the various functional groups have extensively interacted with Ag^+ ions [32,39].

AgNPs antifungal efficiency depends on parameters like shape, size, and surface charge [41]. The smaller-sized

Table 2: Genes of interest, differential expression gene is represented in fragments per kilo base of transcript per million mapped fragments (FPKM) comparing control group vs experimental group

Genes	Control	*C. albicans* + AgNPs	Regulation
ALS1	1,688.46	274.55	Down
ALS3	38.6322	24.6475	
SAP4	12.0663	1.40867	
SAP6	5.35431	1.20598	
PLD1	6.20781	11.0454	Up
PHR1	138.25	461.793	
WH11	24,221.1	36,038	
CDR2	5.81796	16.1013	
ERG3	50.0829	494.461	

AgNPs with spherical forms can have the maximum capacity to release Ag^+ ions due to the larger surface area. The MIC obtained in the present study was 25 $\mu g \cdot mL^{-1}$, similar to the reported in the literature [42] and less than the reports published with the ATCC90028 strain [43]. AgNPs' serial dilutions were tested on *C. albicans* in SDA agar plates, and after 24 h of incubation, it showed no growth. The concentrations of >25 $\mu g \cdot mL^{-1}$ of AgNPs tested were effective as there is no fungal growth, and they did not recover after treatment. Thus, in our study, the particle size plays a vital role in determining its antifungal effect by binding ions to –OH groups and internalizing through the cellular membranes leading to exposed atoms and available for redox reactions and high accumulation of ROS causing damage to nucleic acid leading to apoptosis [25,44,45].

SEM imaging shows a deformed and irregular cell wall when treated with AgNPs. It has been reported that AgNPs can effectively disrupt cell walls creating pits [46,47]. This damage plays an essential role in interaction and adhesion to the host tissue, which is crucial for the first stages of *C. albicans* invasion [48].

HGF and HGF-ATCC were tested for the cytotoxic effect of AgNPs, demonstrating that HGF ATCC was more susceptible to AgNPs than HGF, as reported [49]. It is well known that AgNPs have a cytotoxic effect on several 5human cells [50,51] in a dose-dependent manner, as reported in the present study. Concentrations ranging from 0.0015 to 0.006 $\mu g \cdot mL^{-1}$ exhibited an hormesis effect. In contrast, very low concentrations stimulate cell proliferation interestingly. Some research works have reported that it is due to the activation of the nuclear factor erythroid-derived two related factor 2 (Nrf2) [52]. Pathways of MAPK are involved in the regulation of cell proliferation and the regulation of catabolic pathways during cell stress that translates cell growth, differentiation, and apoptosis [53].

The most expressed gene in *C. albicans* without NPs treatment is the WH11 gene. It is well known that *C. albicans* can switch from white to opaque states. This occurs spontaneously and implicates phenotypic changes in cell wall morphology, size, adhesion to host, and drug susceptibility/resistance [54]. The white states confer the ability to be more virulent than opaque states, which are preferable for rapid multiplication to form biofilm structures [55].

The most expressed genes in *C. albicans* with NPs treatment were more concerning the synthesis of cell wall components such as diacylglycerol (PLD1) that encodes phospholipase, a protein implicated in the change from yeast to hyphae [56]. PHR1 has transferase activity of beta-(1,3)-glucanosyltransferases that is fundamental for cell wall structure. Studies have reported when deletion of this gene in *C. albicans* confers less capacity to adherence to surfaces and epithelial cells [57]. ERG3 chains that it is a protein that catalyzes the induction of C-5 double bond that contributes to the biosynthesis of ergosterol, an essential component of the cell wall [58]. It should be noted that the sequencing

Table 3: Green synthesized AgNPs against different *C. albicans* strains

Reducing agent	AgNPs size (nm)	Strains	References
Rubus fruticosus L. and *Rubus idaeus* L.	25 ± 6	*C. albicans* ATCC 90028	[63]
Argemone mexicana L.	12 ± 8	*C. albicans* ATCC 90028	[64]
Mentha piperita	20	*C. albicans* ATCC 18804	[65]
Furcraea foetida	15	*C. albicans* (183) MTCC	[66]
Anagallis monellin	20 ± 3	*C. albicans* ATCC 90028	[67]
Artemisia annua	10	*C. albicans* ATCC 90028, *C.tropicalis* ATCC 750, *C. glabrata* ATCC 90030	[46]
Limonia acidissima	10–40	*C. albicans* ATCC 90028	[68]
Smilax aspera	12.36	*C. albicans* ATCC 10231	[69]
Ferula pseudalliacea	25 ± 6	*C. albicans* ATTC 90028	[70]

data confirm what was observed in SEM microscopy, where changes in the cell wall were observed in response to oxidative stress; we can confirm that the AgNPs have an oxidation mechanism in *Candida*, as they have also been previously reported. CDR2 encodes a multidrug output transporter that, compared to the genes that were expressed in *Candida* when they were not in contact with the NPs, it is observed that in this condition, it was not expressed, so we conclude that AgNPs caused a toxicity effect that *Candida* recognized as a threat so that it activates the mechanisms similar to those that it activates when in contact with antifungals [59].

In contrast, genes that were less expressed or downregulated are ALS1 and ALS3, a protein necessary for surface adhesion and host invasion [60,61]. Finally, another important family of proteins was notably downregulated: SAP family proteins, such as SAP 4 and 6, are essential as they involve virulence and tissue penetration; it degrades the keratin found in the soft tissues leading to invasion [62]. Several levels of expression of *C. albicans* genes treated with AgNPs are responsible for reducing its effect on the host interaction as a consequence of suppression. Previous studies have reported a change in expression levels of genes associated with cell virulence, adherence, and biofilm formation [63].

5 Conclusions

In the current scenario, many investigations have explored the various biomedical applications of AgNPs and their development as effective antifungal agents. Most studies lack in-depth knowledge on the omic level to elucidate the antimicrobial function. The synthesis of AgNPs assisted with *Pelargonium* leaf extract showed that formed NPs are spherical morphology with an approximate size of 38 nm and high stability. AgNPs showed antifungal effectiveness as a possible solution to the problem of resistance to various therapeutic agents. The overall results from omic profiling show that the expression of genes is upregulated and downregulated, which is of great importance to the virulence, adhesion, and biological activity of *C. albicans* by treating with AgNPs. All of those, as mentioned earlier, suggest a vital role in these genes' cellular response to AgNPs. However, more studies need to be carried out to make the AgNPs with the possible application in biomedicine, especially n-AMBs.

Acknowledgments: Paloma Serrano-Díaz from Programa de Maestría y Doctorado en Ciencias Médicas, Odontológicas y de la Salud, UNAM, would like to acknowledge her CONACyT scholarship (CVU-774685) for her doctoral studies. Also, the authors thank Dr Marina Vega González (SEM analysis) and Lourdes Palma (TEM analysis) for their technical assistance

Funding information: Laura Susana Acosta-Torres acknowledge the financial support from Programa de Apoyo a Proyectos de Investigación e Innovación Tecnológica (PAPIIT) through grant number: IN211922.

Author contributions: Paloma Serrano-Díaz: experimentation, writing – original draft; David W. Williams: methodology, project administration, writing – review and editing; Julio Vega-Arreguin: methodology, formal analysis, writing – review and editing; Ravichandran Manisekaran: writing – original draft, formal analysis, writing – review and editing, data curation; Joshua Twigg: writing – original draft; Daniel Morse: writing – review and editing; René García-Contreras: writing – review and editing; Ma Concepción Arenas-Arrocena: writing – review and editing; Laura Susana Acosta-Torres: writing – review and editing, formal analysis, project administration, resources.

Conflict of interest: Authors state no conflict of interest.

Data availability statement: Available data are presented in the article.

References

[1] Richardson JP. Candida albicans: A major fungal pathogen of humans. Pathogens. 2022;11(4):459. doi: 10.3390/PATHOGENS11040459.

[2] Atiencia-Carrera MB, Cabezas-Mera FS, Tejera E, Machado A. Prevalence of biofilms in Candida spp. bloodstream infections: A meta-analysis. PLoS One. 2022;17(2):e0263522. doi: 10.1371/journal.pone.0263522.

[3] Silva S, Rodrigues CF, Araújo D, Rodrigues ME, Henriques M. Candida species biofilms' antifungal resistance. J Fungi. 2017;3(1):8. doi: 10.3390/jof3010008.

[4] Lohse MB, Gulati M, Johnson AD, Nobile CJ. Development and regulation of single-and multi-species Candida albicans biofilms. Nat Rev Microbiol. 2018;16:19–31. doi: 10.1038/nrmicro.2017.107.

[5] Pohl CH. Recent advances and opportunities in the study of candida albicans polymicrobial biofilms. Front Cell Infect Microbiol. 2022;12:1–17. doi: 10.3389/fcimb.2022.836379.

[6] Pereira R, dos Santos Fontenelle RO, de Brito EHS, de Morais SM. Biofilm of Candida albicans: formation, regulation and resistance. J Appl Microbiol. 2021;131:11–22. doi: 10.1111/jam.14949.

[7] Manisekaran R, García-Contreras R, Chettiar ADR, Serrano-Díaz P, Lopez-Ayuso CA, Arenas-Arrocena MC, et al. 2D

Nanosheets –A new class of therapeutic formulations against cancer. Pharmaceutics. 2021;13:1803. doi: 10.3390/pharmaceutics13111803.
[8] Munir MU, Ahmad MM. Nanomaterials aiming to tackle antibiotic-resistant bacteria. Pharmaceutics. 2022;14(3):582. doi: 10.3390/pharmaceutics14030582.
[9] Garg P, Attri P, Sharma R, Chauhan M, Chaudhary GR. Advances and perspective on antimicrobial nanomaterials for biomedical applications. Front Nanotechnol. 2022;4:1–7. doi: 10.3389/fnano.2022.898411.
[10] Ribeiro AI, Dias AM, Zille A. Synergistic effects between metal nanoparticles and commercial antimicrobial agents: A review. ACS Appl Nano Mater. 2022;5:3030–64. doi: 10.1021/acsanm.1c03891.
[11] Mohammed T, Risan MH, Kadhom M, Raheem R, Yousif E. Antifungal, antiviral, and antibacterial activities of silver nanoparticles synthesized using fungi: A review. Lett Appl NanoBioScience. 2020;9:1307–12. doi: 10.33263/lianbs93.13071312.
[12] Ortega MP, López-Marín LM, Millán-Chiu B, Manzano-Gayosso P, Acosta-Torres LS, García-Contreras R, et al. Polymer mediated synthesis of cationic silver nanoparticles as an effective anti-fungal and anti-biofilm agent against Candida species. Colloids Interface Sci Commun. 2021;43:100449. doi: 10.1016/j.colcom.2021.100449.
[13] Bruna T, Maldonado-Bravo F, Jara P, Caro N. Silver nanoparticles and their antibacterial applications. Int J Mol Sci. 2021;22(13):7202. doi: 10.3390/ijms22137202.
[14] Anees Ahmad S, Sachi Das S, Khatoon A, Tahir Ansari M, Afzal M, Saquib Hasnain M, et al. Bactericidal activity of silver nanoparticles: A mechanistic review. Mater Sci Energy Technol. 2020;3:756–69. doi: 10.1016/j.mset.2020.09.002.
[15] Liu RH, Shang ZC, Li TX, Yang MH, Kong LY. In vitro antibiofilm activity of eucarobustol E against Candida albicans. Antimicrob Agents Chemother. 2017;61(8):e02707–16. doi: 10.1128/AAC.02707-16.
[16] Zheng X, Wang J, Chen Y, Wei Y. Comprehensive analysis of transcriptional and proteomic profiling reveals silver nanoparticles-induced toxicity to bacterial denitrification. J Hazard Mater. 2018;344:291–8. doi: 10.1016/j.jhazmat.2017.10.028.
[17] Piersanti A, Juganson K, Mozzicafreddo M, Wei W, Zhang J, Zhao K, et al. Transcriptomic responses to silver nanoparticles in the freshwater unicellular eukaryote Tetrahymena thermophila. Env Pollut. 2021;269:115965. doi: 10.1016/j.envpol.2020.115965.
[18] Sun D, Zhang W, Mou Z, Chen Y, Guo F, Yang E, et al. Transcriptome analysis reveals silver nanoparticle-decorated quercetin antibacterial molecular mechanism. ACS Appl Mater Interfaces. 2017;9:10047–60. doi: 10.1021/acsami.7b02380.
[19] Singh S, Bharti A, Meena VK. Structural, thermal, zeta potential and electrical properties of disaccharide reduced silver nanoparticles. J Mater Sci Mater Electron. 2014;25:3747–52. doi: 10.1007/s10854-014-2085-x.
[20] Horstmann C, Campbell C, Kim DS, Kim K. Transcriptome profile with 20 nm silver nanoparticles in yeast. FEMS Yeast Res. 2019;19:1–15. doi: 10.1093/femsyr/foz003.
[21] Masri A, Khan NA, Zoqratt MZHM, Ayub Q, Anwar A, Rao K, et al. Transcriptome analysis of Escherichia coli K1 after therapy with hesperidin conjugated with silver nanoparticles. BMC Microbiol. 2021;21(1):1. doi: 10.1186/s12866-021-02097-2.
[22] Gliga AR, Di Bucchianico S, Lindvall J, Fadeel B, Karlsson HL. RNA-sequencing reveals long-term effects of silver nanoparticles on human lung cells. Sci Rep. 2018;8(1):6668. doi: 10.1038/s41598-018-25085-5.
[23] Adam RZ, Khan SB. Antimicrobial efficacy of silver nanoparticles against Candida albicans: A systematic review protocol. PLoS One. 2021;16(1):e0245811. doi: 10.1371/journal.pone.0245811.
[24] Amelia Piñón Castillo H, Nayzzel Muñoz Castellanos L, Martínez Chamorro R, Reyes Martínez R, Orrantia Borunda E. Nanoparticles as new therapeutic agents against Candida albicans. Candida Albicans. London, UK: IntechOpen; 2019. doi: 10.5772/intechopen.80379.
[25] Ihsan M, Niaz A, Rahim A, Zaman MI, Arain MB, Sharif T, et al. Biologically synthesized silver nanoparticle-based colorimetric sensor for the selective detection of Zn2+. RSC Adv. 2015;5:91158–65. doi: 10.1039/c5ra17055a.
[26] Raj S, Trivedi R, Soni V. Biogenic synthesis of silver nanoparticles, characterization and their applications—A review. Surfaces. 2021;5:67–90. doi: 10.3390/surfaces5010003.
[27] Alsubki R, Tabassum H, Abudawood M, Rabaan AA, Alsobaie SF, Ansar S. Green synthesis, characterization, enhanced functionality and biological evaluation of silver nanoparticles based on Coriander sativum. Saudi J Biol Sci. 2021;28:2102–8. doi: 10.1016/j.sjbs.2020.12.055.
[28] Devi HS, Boda MA, Shah MA, Parveen S, Wani AH. Green synthesis of iron oxide nanoparticles using Platanus orientalis leaf extract for antifungal activity. Green Process Synth. 2019;8:38–45. doi: 10.1515/gps-2017-0145.
[29] Elgorban AM, Al-Rahmah AN, Sayed SR, Hirad A, Mostafa AAF, Bahkali AH. Antimicrobial activity and green synthesis of silver nanoparticles using Trichoderma viride. Biotechnol Biotechnol Equip. 2016;30:299–304. doi: 10.1080/13102818.2015.1133255.
[30] Swilam N, Nematallah KA. Polyphenols profile of pomegranate leaves and their role in green synthesis of silver nanoparticles. Sci Rep. 2020;10:14851. doi: 10.1038/s41598-020-71847-5.
[31] Alwhibi MS, Soliman DA, Awad MA, Alangery AB, Al Dehaish H, Alwasel YA. Green synthesis of silver nanoparticles: Characterization and its potential biomedical applications. Green Process Synth. 2021;10:412–20. doi: 10.1515/gps-2021-0039.
[32] Al Masud MA, Shaikh H, Alam MS, Karim MM, Momin MA, Islam MA, et al. Green synthesis of silk sericin-embedded silver nanoparticles and their antibacterial application against multidrug-resistant pathogens. J Genet Eng Biotechnol. 2021;19(1):1. doi: 10.1186/s43141-021-00176-5.
[33] Rónavári A, Igaz N, Adamecz DI, Szerencsés B, Molnar C, Kónya Z, et al. Green silver and gold nanoparticles: Biological synthesis approaches and potentials for biomedical applications. Molecules. 2021;26(4):844. doi: 10.3390/molecules26040844.
[34] Mohammadlou M, Jafarizadeh-Malmiri H, Maghsoudi H. Hydrothermal green synthesis of silver nanoparticles using Pelargonium/Geranium leaf extract and evaluation of their antifungal activity. Green Process Synth. 2017;6:31–42. doi: 10.1515/gps-2016-0075.

[35] Wang M, Li H, Li Y, Mo F, Li Z, Chai R, et al. Dispersibility and size control of silver nanoparticles with anti-algal potential based on coupling effects of polyvinylpyrrolidone and sodium tripolyphosphate. Nanomaterials. 2020;10(6):1042. doi: 10.3390/nano10061042.
[36] Bamal D, Singh A, Chaudhary G, Kumar M, Singh M, Rani N, et al. Silver nanoparticles biosynthesis, characterization, antimicrobial activities, applications, cytotoxicity and safety issues: An updated review. Nanomaterials. 2021;11(8):2086. doi: 10.3390/nano11082086.
[37] Raja S, Ramesh V, Thivaharan V. Green biosynthesis of silver nanoparticles using Calliandra haematocephala leaf extract, their antibacterial activity and hydrogen peroxide sensing capability. Arab J Chem. 2017;10:253–61. doi: 10.1016/j.arabjc.2015.06.023.
[38] Ahmed S, Saifullah, Ahmad M, Swami BL, Ikram S. Green synthesis of silver nanoparticles using Azadirachta indica aqueous leaf extract. J Radiat Res Appl Sci. 2016;9:1–7. doi: 10.1016/j.jrras.2015.06.006.
[39] Mickymaray S. One-step synthesis of silver nanoparticles using saudi arabian desert seasonal plant Sisymbrium irio and antibacterial activity against multidrug-resistant bacterial strains. Biomolecules. 2019;9(11):662. doi: 10.3390/biom9110662.
[40] Gibała A, Żeliszewska P, Gosiewski T, Krawczyk A, Duraczyńska D, Szaleniec J, et al. Antibacterial and antifungal properties of silver nanoparticles – effect of a surface-stabilizing agent. Biomolecules. 2021;11(10):1481. doi: 10.3390/biom11101481.
[41] Mansoor S, Zahoor I, Baba TR, Padder SA, Bhat ZA, Koul AM, et al. Fabrication of silver nanoparticles against fungal pathogens. Front Nanotechnol. 2021;3:679358. doi: 10.3389/fnano.2021.679358.
[42] Onodera A, Nishiumi F, Kakiguchi K, Tanaka A, Tanabe N, Honma A, et al. Short-term changes in intracellular ROS localisation after the silver nanoparticles exposure depending on particle size. Toxicol Rep. 2015;2:574–9. doi: 10.1016/j.toxrep.2015.03.004.
[43] Tian W, Li F, Wu S, Li G, Fan L, Qu X, et al. Efficient capture and T2 magnetic resonance assay of candida albicans with inorganic nanoparticles: Role of nanoparticle surface charge and fungal cell wall. ACS Biomater Sci Eng. 2019;5:3270–8. doi: 10.1021/acsbiomaterials.9b00069.
[44] Koduru JR, Kailasa SK, Bhamore JR, Kim KH, Dutta T, Vellingiri K. Phytochemical-assisted synthetic approaches for silver nanoparticles antimicrobial applications: A review. Adv Colloid Interface Sci. 2018;256:326–39. doi: 10.1016/j.cis.2018.03.001.
[45] Ahmed S, Ahmad M, Swami BL, Ikram S. A review on plants extract mediated synthesis of silver nanoparticles for antimicrobial applications: A green expertise. J Adv Res. 2016;7:17–28. doi: 10.1016/j.jare.2015.02.007.
[46] Khatoon N, Sharma Y, Sardar M, Manzoor N. Mode of action and anti-Candida activity of Artemisia annua mediated-synthesized silver nanoparticles. J Mycol Med. 2019;29:201–9. doi: 10.1016/j.mycmed.2019.07.005.
[47] Gulati M, Nobile CJ. Candida albicans biofilms: development, regulation, and molecular mechanisms. Microbes Infect. 2016;18:310–21. doi: 10.1016/j.micinf.2016.01.002.
[48] Thonemann B, Schmalz G, Hiller KA, Schweikl H. Responses of L929 mouse fibroblasts, primary and immortalized bovine dental papilla-derived cell lines to dental resin components. Dental Mater. 2002;18(4):318–23. doi: 10.1016/S0109-5641(01)00056-2.
[49] Liao C, Li Y, Tjong SC. Bactericidal and cytotoxic properties of silver nanoparticles. Int J Mol Sci. 2019;20(2):449. doi: 10.3390/ijms20020449.
[50] Das G, Patra JK, Shin HS. Biosynthesis, and potential effect of fern mediated biocompatible silver nanoparticles by cytotoxicity, antidiabetic, antioxidant and antibacterial, studies. Mater Sci Eng C. 2020;114:111011. doi: 10.1016/j.msec.2020.111011.
[51] Sthijns MM, Thongkam W, Albrecht C, Hellack B, Bast A, Haenen GR, et al. Silver nanoparticles induce hormesis in A549 human epithelial cells. Toxicol Vitr. 2017;40:223–33. doi: 10.1016/j.tiv.2017.01.010.
[52] Jiao ZH, Li M, Feng YX, Shi JC, Zhang J, Shao B. Hormesis effects of silver nanoparticles at non-cytotoxic doses to human hepatoma cells. PLoS One. 2014;9(7):e102564. doi: 10.1371/journal.pone.0102564.
[53] Srikantha T, Chandrasekhar A, Soll DR. Functional analysis of the promoter of the phase-specific WH11 gene of Candida albicans. 1995;15(3):1797–805. doi: 10.1128/mcb.15.3.1797.
[54] Zordan RE, Galgoczy DJ, Johnson AD. Epigenetic properties of white-opaque switching in Candida albicans are based on a self-sustaining transcriptional feedback loop. Proc Natl Acad Sci U S A. 2006;103:12807–12. doi: 10.1073/pnas.0605138103.
[55] Dolan JW, Bell AC, Hube B, Schaller M, Warner TF, Balish E. Candida albicans PLDI activity is required for full virulence. Med Mycol. 2004;42:439–47. doi: 10.1080/13693780410001657162.
[56] Calderon J, Zavrel M, Ragni E, Fonzi WA, Rupp S, Popolo L. PHR1, a pH-regulated gene of Candida albicans encoding a glucan-remodelling enzyme, is required for adhesion and invasion. Microbiology. 2010;156:2484–94. doi: 10.1099/mic.0.038000-0.
[57] Hirayama T, Miyazaki T, Sumiyoshi M, Ashizawa N, Takazono T, Yamamoto K, et al. ERG3-encoding sterol C5,6-DESATURASE in Candida albicans Is required for virulence in an enterically infected invasive candidiasis mouse model. Pathogens. 2021;10:1–9. doi: 10.3390/pathogens10010023.
[58] Niimi K, Maki K, Ikeda F, Holmes AR, Lamping E, Niimi M, et al. Overexpression of Candida albicans CDR1, CDR2, or MDR1 does not produce significant changes in echinocandin susceptibility. Antimicrob Agents Chemother. 2006;50:1148–55. doi: 10.1128/AAC.50.4.1148-1155.2006.
[59] Ho V, Herman-Bausier P, Shaw C, Conrad KA, Garcia-Sherman MC, Draghi J, et al. An amyloid core sequence in the major Candida albicans adhesin Als1p mediates cell-cell adhesion. MBio. 2019;10(5):e01766-19. doi: 10.1128/mBio.01766-19.
[60] Hoyer LL, Cota E. Candida albicans agglutinin-like sequence (Als) family vignettes: A review of als protein structure and function. Front Microbiol. 2016;7:280. doi: 10.3389/fmicb.2016.00280.
[61] Kadry AA, El-Ganiny AM, El-Baz AM. Relationship between sap prevalence and biofilm formation among resistant clinical isolates of candida albicans. Afr Health Sci. 2018;18:1166–74. doi: 10.4314/AHS.V18I4.37.

[62] Wunnoo S, Paosen S, Lethongkam S, Sukkurd R, Waengoen T, Nuidate T, et al. Biologically rapid synthesized silver nanoparticles from aqueous Eucalyptus camaldulensis leaf extract: Effects on hyphal growth, hydrolytic enzymes, and biofilm formation in Candida albicans. Biotechnol Bioeng. 2021;118:1597–611. doi: 10.1002/bit.27675.

[63] Ekrikaya S, Yilmaz E, Celik C, Demirbuga S, Ildiz N, Demirbas A, et al. Investigation of ellagic acid rich-berry extracts directed silver nanoparticles synthesis and their antimicrobial properties with potential mechanisms towards Enterococcus faecalis and Candida albicans. J Biotechnol. 2021;341:155–62. doi: 10.1016/j.jbiotec.2021.09.020.

[64] Téllez-de-Jesús DG, Flores-Lopez NS, Cervantes-Chávez JA, Hernández-Martínez AR. Antibacterial and antifungal activities of encapsulated Au and Ag nanoparticles synthesized using Argemone mexicana L extract, against antibiotic-resistant bacteria and Candida albicans. Surf Interfaces. 2021;27:101456. doi: 10.1016/j.surfin.2021.101456.

[65] Robles-Martínez M, Patiño-Herrera R, Pérez-Vázquez FJ, Montejano-Carrizales JM, González JFC, Pérez E. Mentha piperita as a natural support for silver nanoparticles: A new Anti-Candida albicans treatment. Colloids Interface Sci Commun. 2020;35:100253. doi: 10.1016/j.colcom.2020.100253.

[66] Sitrarasi R, Nallal VUM, Razia M, Chung WJ, Shim J, Chandrasekaran M, et al. Inhibition of multi-drug resistant microbial pathogens using an eco-friendly root extract of Furcraea foetida mediated silver nanoparticles. J King Saud Univ - Sci. 2022;34:101794. doi: 10.1016/j.jksus.2021.101794.

[67] Shaheena S, Chintagunta AD, Dirisala VR, Kumar NSS. Extraction of bioactive compounds from Psidium guajava and their application in dentistry. AMB Express. 2019;9(1):208. doi: 10.1186/s13568-019-0935-x.

[68] Kanchana P, Hemapriya V, Arunadevi N, Shanmuga S, Chung I, Prabakaran M. Phytofabrication of silver nanoparticles from Limonia acidissima leaf extract and their antimicrobial, antioxidant and its anticancer prophecy. J Indian Chem Soc. 2022;99:100679. doi: 10.1016/j.jics.2022.100679.

[69] Negi A, Vishwakarma RK, Negi DS. Synthesis and evaluation of antibacterial, anti-fungal, anti-inflammatory properties of silver nanoparticles mediated via roots of Smilax aspera. Mater Today Proc. 2022;57:27–33. doi: 10.1016/j.matpr.2022.01.203.

[70] Kocak Y, Oto G, Meydan I, Seckin H, Gur T, Aygun A, et al. Assessment of therapeutic potential of silver nanoparticles synthesized by Ferula Pseudalliacea rech. F. plant. Inorg Chem Commun. 2022;140:109417. doi: 10.1016/j.inoche.2022.109417.